A Theoretical Investigation of the Ground and Excited States of Selected Ru and Os Polypyridyl Molecular Dyes

Jean-François Guillemoles,[†] Vincenzo Barone,[‡] Laurent Joubert,[†] and Carlo Adamo*[,†]

Ecole Nationale Supérieure de Chimie de Paris, Laboratoire d'Electrochimie et Chimie Analytique, UMR CNRS-ENSCP no. 7575, 11 rue P. et M. Curie, F-75231 Paris Cedex 05, France, and Dipartimento di Chimica, Università degli Studi di Napoli "Federico II", Complesso Monte S. Angelo, Via Cintia, I-80126 Napoli, Italy

Received: June 28, 2002; In Final Form: September 9, 2002

Density functional theory (DFT) is applied to analyze ground and excited-state properties of some $M(bpy)_2L_2$ complexes (M = Ru, Os, L = CN, SCN, bpy = 2,2′-bipyridine), both in the gas phase and in aqueous solution. In particular, vertical excitation energies were computed by the PBEO hybrid functional in the framework of a time dependent DFT (TDDFT) approach, whereas the polarizable continuum model (PCM) was used to take into account solvent effects. Our results in the gas phase show that the PBE0 functional provides accurate description of all the low lying electronic states considered and correctly reproduces the excitation spectra of such complexes. Some insights on the difference observed for these complexes in changing the central metal atom, the chemical environment, or the medium are given.

1. Introduction

Metal based dyes, and especially those containing pyridyl ligands, have proven to be very effective in photocatalysis and in photovoltaic conversion.[1] They have also shown good luminescence and electroluminescence abilities, with performances approaching those of more traditional solid-state semiconducting devices.[2,3] They are also in the core of molecules investigated for molecular electronics (molecular wires, molecular switches) or as prototypes of the so-called "molecular machines".[4] Their peculiar molecular properties, and the possibilities of related technological applications, are directly related to (a) the energetic spectrum of the molecules that determines the optical absorption and emission characteristics and (b) the molecular electronic structure of the ground as well as of the lowest excited states.

From the point of view of potential industrial applications, these properties are especially important for the conversion of solar energy using dye sensitized mesoporous TiO_2 in photoelectrochemical cells. In this case, the dye is present as a monolayer at the interface between a semiconductor surface (TiO_2) and an electrolyte containing a redox couple. In such systems, photons have to be absorbed efficiently by the dye, and the excited electron is injected very quickly into the semiconductor while the dye is regenerated by a redox couple such as I_3^-/I_2. Working principles of these devices have been exposed in many articles and reviews (see for instance refs 5 and 6). From a mechanistic point of view, the electronic characteristics of the dyes are strongly linked to the ability of the molecules to inject (or accept) electrons to (or from) the surface or to redox species, a property most desirable for its photochemical or optoelectronic applications. Furthermore, photovoltaic applications require the absorption spectrum of the dye matches the solar one as closely as possible or that it should be adapted to other devices such as electroluminescent diodes. A high absorption coefficient is also preferable for such devices because this reduces the amount of dye for a given photocurrent and could in principle lead to cheaper and more efficient solar cells.

Metal based dyes have proven to perform surprisingly well, and against all odds, some dye molecules were found to be very stable under operating conditions.[6] Among the puzzles of these systems, we recall the efficient and very fast injection of electrons in some semiconductors such as TiO_2, the conformation of the excited state and the explanation for the exceptional stability of the excited state of the dye, especially after the loss of an electron.[7−10]

Surprisingly, very little theoretical work is available on this topic despite the potential interest of an advanced quantum chemical approach for a better understanding of key issues, like the nature of both the ground and the excited states involved in the absorption and/or photoemission and its tuning by environmental (solvent and/or crystal) effects. As a matter of fact, even if great attention has been devoted to the $[Ru(2,2'\text{-bipyridine})_3]^{2+}$ complex (see for instance refs 11 and 12), other molecules belonging to the same family have been only scarcely analyzed.[13−17]

The main difficulties against a reliable computational approach are related to the size of such systems and to the presence of strong electron correlation effects. Both properties are difficult to treat in the framework of the quantum mechanical methods rooted in the Hartree−Fock (HF) theory. As a matter of fact, the post-Hartree−Fock methods needed to obtain reliable excited states properties have scaling properties with the number of electrons (N^6 or worse) that prevent their application to large systems. This can explain why even recent investigations have been carried out at the approximate level of theory (semiempirical models)[13,14,17] or with quite crude model systems, obtained by a reduction of the size of the system under investigation.[15]

On the other hand, density functional theory (DFT) has been remarkably successful at providing a means to evaluate a variety

* Corresponding author. E-mail: adamo@ext.jussieu.fr.
† ENSCP.
‡ Università Federico II.

10.1021/jp021517v CCC: $22.00
Published on Web 10/26/2002

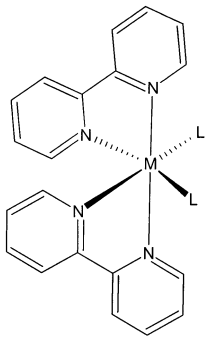

Figure 1. Sketches of the considered Ru and Os complexes.

of ground-state properties with an accuracy close to that of post-HF methods.[18,19] As a consequence, there is currently a great interest in extending DFT to excited electronic states.[20] In this context, the time dependent DFT approach (TDDFT) offers a rigorous route to the calculation of vertical electronic excitation spectra.[21−23] Several tests have shown that standard approaches, including hybrid HF/DFT methods, provide results for low excitation energies usually superior to those obtained by time-dependent HF methods, or by the configuration interaction with singles excitations CIS approach.[24−27] In particular, we have recently introduced the so-called PBE0 model, a hybrid HF/DFT approach based on the Perdew−Burke−Erzenrhof (PBE) functional.[28,29] This approach overcomes many of the problems encountered with standard functionals, providing accurate excitation energies to both valence and Rydberg states.[30,31] Furthermore, we have showed that even charge transfer (CT) bands in metal complexes are well reproduced in the gas phase[32] and even in solution.[33]

In this paper we endeavored to show how the contemporary improvements in model density functionals result in a powerful and effective computational tool for the study of a family of derivatives that is central to the field of photochemistry. To this end, we have studied the structure and electronic properties of the ground and lowest excited states of a family of metal polypyridyl complexes, namely *cis*-M(bpy)$_2$L$_2$ (M = Ru, Os, L = CN and SCN, and bpy = 2,2′-bipyridine; see Figure 1).

These molecules, used as photosensitizers in TiO_2 based solar cells,[10,33] have achieved an extremely high energy conversion (up to 10%) for a photovoltaic system based on organic molecules.[34] For these reasons, such Ru and Os complexes have already been the subject of a detailed analysis of structural, electronic, and optical properties at the experimental level.[35−38]

The aim of this paper is 2-fold. On the one hand, we want to gain information on the physicochemical characteristics of the ground and low lying excited states and, in particular, to understand the role of the central metal atom and of its chemical environment in tuning the dye properties. On the other hand, we want to show the potential of a quantum mechanical modeling based on DFT, in the evaluation of ground and excited state properties by comparison to the available experimental data.

2. Computational Details

All DFT calculations were carried out with a development version of the Gaussian code,[39] using a recent model referred to as PBE0,[29]. This approach is obtained by casting the PBE exchange and correlation functionals[28] in a hybrid HF/DFT scheme, where the HF exchange ratio (1/4) is fixed a priori.[40]

All systems have been fully optimized (in C_2 symmetry) at the PBE0 level, using the CEP-121 pseudopotentials and the corresponding basis set for Os and Ru atoms, and the 6-31G(d) basis set for all the other atoms.[41] A larger basis set has been used for TDDFT computations, taking the 6-31+G(d,p) basis sets for the lighter atoms and adding one p polarization function (exp = 0.08) to the CEP-121 basis for the metal atoms.[42] Unrestricted calculations were performed for triplet states.

Solvent effects were evaluated using the polarizable continuum model (PCM).[43] In particular, optimized structures and solvation energies have been computed by a cavity model, namely the united atoms topological model (UATM),[44] coupled to the conductor-like polarizable continuum model (CPCM).[45] This approach provides results very close to those obtained by the original dielectric model for high dielectric constant solvents, but it is significantly more effective in geometry optimizations, and less prone to numerical errors arising from the small part of the solute electron cloud lying outside the cavity (escaped charge effects).[45] Solvent shifts of excitation bands were evaluated by a recent nonequilibrium implementation[46] of the polarizable continuum model (in its CPCM version).

Finally, the electronic structure of these molecules have been investigated using the "atoms in molecule" (AIM) approach.[47] According to this theory, topological atoms are defined as regions in real space consisting of a bundle of electron density gradient paths attracted to a nucleus. This partition allows evaluating atomic properties, defined as volume integrals over nonoverlapping atomic basins. In particular, the population associated with an atom is the volume integral of $\rho(\mathbf{r})$ over the basin. All these topological calculations have been performed with the Topmod package.[48]

3. Results and Discussion

As mentioned in the Introduction, we have analyzed in detail the ground state (S0) and the first excited singlet electronic states (S1), as well as the lowest triplet (T1) for all the considered *cis*-M(bpy)$_2$L$_2$ complexes. Although the understanding of the ground electronic states in these metal polypyridyl complexes can lead to some insights into the redox mechanism taking place in solution or at the surface of the semiconductor,[1] excited states are directly involved in the primary steps of the photovoltaic process, light absorption and charge transfer. Thus an understanding of the lowest excited states and of how their characteristics depend on the chemical environment (solvent, ligands) is of great interest also for technological applications. In particular, the lowest triplet state has been detected as an intermediate either in absorption or emission of osmium complexes.[36,49] Some of these computations have been carried out using the CPCM to model the solvent (water) effects on the dyes. Because photoelectrodes often contain water as electrolyte, we limit the present study to this solvent, known to give spectra blue-shifted as compared to less-polar organic solvent.[5,37]

3.1. Ground Electronic State. The optimized geometrical parameters, computed both in the gas phase and in aqueous solution, for all the molecules considered are reported in Tables 1 and 2, together with the available X-ray data.[37,50] The atom labeling is reported in Figure 2. Before discussing in detail these results, we want to point out that the linkage isomerization of the thiocyanate complexes in solution or at TiO_2 surfaces is still a matter of debate.[51] Here, we have followed recent NMR

TABLE 1: Main Geometrical Parameters (Ångstroms and Degrees) of the Singlet Ground State of the $M(bpy)_2CN_2$ (M = Ru and Os) Complexes[a]

	M = Ru			M = Os	
$M(bpy)_2CN_2$	gas phase	exp[b]	aq soln	gas phase	aq soln
MN2	2.109	2.108	2.122	2.089	2.115
C1N2	1.360	1.335	1.369	1.365	1.365
N2C3	1.376	1.350	1.380	1.381	1.378
C3C4	1.476	1.481	1.481	1.468	1.476
C4N5	1.379	1.365	1.384	1.385	1.381
N5C6	1.365	1.334	1.371	1.371	1.367
MN5	2.069	2.051	2.090	2.051	2.075
MC7	2.020	1.991	1.945	2.011	1.991
C7N8	1.195	1.146	1.169	1.195	1.197
MN2C3	115.4	114.9	115.4	116.1	115.4
MN2C1	125.6	126.7	125.8	125.2	125.9
MN5C4	116.6	116.0	116.2	117.2	116.6
MN5C6	124.3	125.6	125.3	124.3	124.6
C7MN5	93.7	97.3	94.8	93.5	94.0
N2C3C4N5	0.4	2.7	0.3	0.5	0.3

[a] All values have been computed at the PBE0 level using the CEP-121G basis. [b] Reference 54.

TABLE 2: Main Geometrical Parameters (Ångstroms and Degrees) of the Singlet Ground State of the $M(bpy)_2NCS_2$ (M = Ru and Os) Complexes[a]

	M = Ru			M = Os	
$M(bpy)_2NCS_2$	gas phase	aq soln	exp[b]	gas phase	aq soln
MN2	2.060	2.147	2.046(16)	2.032	2.086
C1N2	1.362	1.368	1.351 (21)	1.370	1.374
N2C3	1.380	1.381	1.383(18)	1.387	1.388
C3C4	1.475	1.488	1.487(19)	1.460	1.480
C4N5	1.380	1.387	1.379 (20)	1.383	1.388
N5C6	1.361	1.374	1.353(19)	1.367	1.377
MN5	2.059	2.134	2.030(13)	2.048	2.082
MN7	2.042	1.924	2.046(16)	2.023	1.928
N7C8	1.195	1.177	1.162(21)	1.195	1.164
C8S9	1.685	1.663	1.685 (22)	1.679	1.689
MN2C3	115.5	115.1		116.3	115.7
MN2C1	125.6	126.2	125.4(20)	125.3	126.0
MN5C4	115.6	115.1	114.5(9)	116.0	115.8
MN5C6	124.5	126.4	125.0(11)	124.7	126.8
N7MN5	94.1	97.8	95.9(5)	94.4	93.7
N2C3C4N5	1.8	1.1		1.6	0.6

[a] All values have been computed at the PBE0 level using the CEP-121G basis. [b] Reference 38.

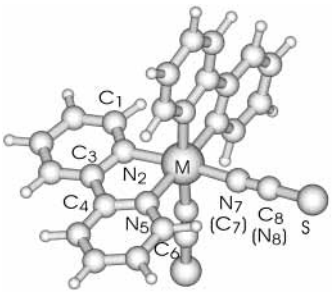

Figure 2. Structure and atom labeling for the $M(bpy)_2(NCS)_2$ (M = Os, Ru) complexes. In parentheses are reported the labels for the corresponding $M(bpy)_2(CN)_2$ compounds.

indications and X-ray data supporting the hypothesis that the most stable isomer involves N-bonding.[36−38]

There is an overall satisfactory agreement between the theoretical and the available experimental data. All the computed distances are within the experimental error (±0.03 Å). This accuracy is the one expected for the method, taking also into account experimental factors (e.g., crystal packing forces) that occasionally can be responsible for apparent discrepancies.

As a general remark, we can note that the corresponding complexes of Ru and Os have very similar geometrical rearrangements, the largest differences (max 0.02 Å) concerning the bonds to the central metal atom. Because the pseudopotentials and the corresponding basis sets for the two atoms have been generated with the same approach, this small effect can be attributed to different orbital interactions. In a simple Dewar, Chatt, and Duncanson model,[52,53] the bonding interaction can be described as a donation from a σ molecular orbital of the ligand (i.e., CN^- or SCN^-) toward an empty d_σ orbital of the metal and a concurrent back-donation from a filled (or partially filled) d_π orbital to a π^* antibonding orbital of the ligand. In the $M(bpy)_2^{2+}$ fragment, for instance, the lowest unoccupied molecular orbital (LUMO) has, not surprisingly, the same energy for both Os and Ru compounds (about −9.8 eV), and therefore cannot be responsible for the observed differences. On the other hand, there is a small variation in energy between the doubly occupied d_π orbitals (0.3 eV), the one of Os being higher in energy. As a consequence, the d_π orbital of $Os(bpy)_2^{2+}$ lies closer in energy to the π^* antibonding orbital of cyanide. This small difference, together with the fact that the 4d's of Ru, being less diffuse than the 5d's of Os, provide a smaller overlap with the molecular orbitals of the ligand, can explain the difference found in the geometrical parameters. The same principles are, of course, at work in the case of SCN^- and for the bipyridyl ligand. We want also to notice that the above-discussed difference (0.3 eV) is in good agreement with the measured difference in standard potentials of oxidation of the two complexes.[36]

It is interesting to note the relative effects on the geometrical parameters in going from cyanide to thiocyanate. Essentially, the distance between the metal atom and the ligand is shorter for CN^- than NCS^-. This is consistent with the idea that CN^- is a better donor than NCS^- and, so, more prone to share electrons for bonding. At the same time, there is a stronger trans effect on the bypyridyl moiety for the CN than for the NCS group, the M−N distance being longer for the first complexes than for the second ones. The two effects are, of course, concurrent.

In going from the gas phase to the aqueous solution, a general contraction of all the metal−ligand (CN^- or SCN^-) bond lengths is observed, about 3 times larger for the Ru complexes than for the Os analogues. At the same time, solvent effects are larger on the more polarizable thiocyanate anion than on the harder cyanide. Both effects correspond, in turn, to an increase of the metal−bypiridine distance in all complexes. They are larger in the thiocyanate than in the cyanide containing compounds. Bipyridyl parameters are, instead, practically unaffected by the solvent reaction field. These geometrical variations are consistent with the stabilization of structures involving a formal charge separation (like $M(bpy)_2^{2+}-L^{2-}$) by polar solvents.

Some insights on the electronic structures of such complexes can be obtained by looking at the AIM charges, calculated both in vacuo and in solution and reported in Table 3. Taking as reference the bare fragments, i.e., $M(bpy)_2^{2+}$ and CN^-, the charge transferred from each of the anions to the metal is similar for the two metals, namely about 0.35 $|e^-|$. The small discrepancy observed (0.02 $|e^-|$) is an evidence of a slightly stronger $Os(d_\pi) \rightarrow CN(\pi^*)$ back-donation, in agreement with our orbital analysis. In contrast, it is worth noting the substantial variations of metal charge, from +1.16 $|e^-|$ for Ru to +1.33 $|e^-|$ for the Os complex. This latter fact reflects the shorter metal−bipyridyl distance found for the Os complex, and suggests a stronger back-donation to the π^* orbital of the bidentate ligand.

TABLE 3: AIM Charges for the Singlet Ground State of the All Considered Complexes[a]

	$M(bpy)_2(CN)_2$		$M(bpy)_2(NCS)_2$	
	gas phase	soln	gas phase	soln
Ru	1.16	1.14	1.35	1.31
bpy	0.06	0.18	0.08	0.18
L	−0.64	−0.75	−0.75	−0.84
Os	1.33	1.28	1.55	1.51
bpy	−0.01	0.13	0.02	0.10
L	−0.66	−0.77	−0.76	−0.86

[a] All the values have been computed in gas phase and in aqueous solution at the PBE0 level, using the CEP-121 basis set and the corresponding optimized geometries.

Similar trends are found for the thiocyanate complexes but with different magnitudes. For these systems, anion-to-metal charge transfers decrease by approximately 0.1 $|e^-|$ compared to their cyanide analogues. Accordingly, the positive charge localized on the metal increases, the difference between Ru (+1.35) and Os (+1.55) remaining constant.

As mentioned above, the solvent increases the charge separation in the complex, significantly reducing the charge transferred from the cyanide or thiocyanate group to the metal complexes. For instance, the charge transferred from the cyanide is 0.25 $|e^-|$ in the Ru complex and 0.23 $|e^-|$ in the Os analogous, whereas an even smaller transfer is found for the thyocyanide complex (0.16 and 0.14 $|e^-|$ for Ru and Os, respectively). Furthermore, AIM charges of the Ru and Os atom slightly decrease, whereas larger positive charges are localized on the bidentate ligands. For Ru derivatives, the metal charge is +1.14 $|e^-|$ for the cyanide containing complex and +1.28 $|e^-|$ for the thiocyanate one, whereas the corresponding charges on the bipyridine are +0.18 and +0.13 $|e^-|$, respectively. Similar variations are found for the Os compounds. These effects underline a stronger electron donation from the bypirydyl ring. In short, the solvent, stabilizing the polar form $M(bpy)_2^{2+}-L^{2-}$, induces a strong electronic rearrangement, ruled by an increase of the electron donation from bipyridine to metal and by a weakening of the covalent character of the metal−cyanide/thiocyanate interaction.

Frontier orbitals play a relevant role in such systems, because they rule the redox reaction in which the dyes are involved during or after the electronic excitations.[1] The highest occupied molecular orbitals (HOMO) and the LUMO have similar features in all the considered complexes, as can be seen from the sketches of Figure 3. As expected, the HOMO has a strong d-metal character, but significant contributions come from the p orbitals of the more external atoms of cyanide or thyocianide ligands (N and S, respectively). These contributions might have a relevant role in the whole photovoltaic cycle. In fact, in a photovoltaic cell, the oxidized dye, after electron injection to the conduction band of the oxide, is quickly reduced by a redox species in the surrounding electrolyte. Therefore, the fact that the HOMO contains a contribution from the external S or N atoms, may favor the regeneration of the photochemical properties of the dye.[6] In contrast, the LUMO is essentially a π^* orbital localized on the bipyrdil ligand, thus all the active transitions to this last orbital can be described as metal to ligand charge transfer (MLCT) bands (vide infra).

3.2. Lowest Triplet States. The lowest triplet state, T1, has been analyzed by carrying out unrestricted PBE0 calculations both at the corresponding S0 geometries and at the fully optimized triplet structure. The calculated energy gaps with respect to the ground electronic state are reported in Table 4. They have been computed both as energy difference with respect to S0 (the so-called ΔSCF approach) and by the TDDFT approach. In all the considered complexes, the triplet state corresponds to an excitation from the HOMO to the LUMO (see Figure 3). The spin density map for the *cis*-$Ru(bpy)_2(CN)_2$ complex, reported in Figure 4, shows well the sharing of the two unpaired electrons between the metal (d orbital) and the pyridyl ligand (π^* orbital), with smaller contributions from the external nitrogen atoms. Of course, similar behaviors have been found for all the other complexes.

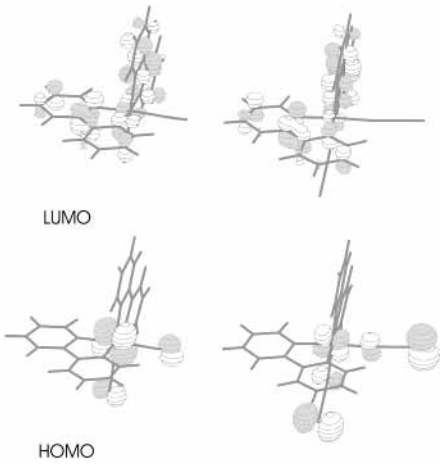

Figure 3. Schematic drawings of the frontier orbitals for $Ru(bpy)_2(CN)_2$ (left) and $Ru(bpy)_2(NCS)_2$ (right).

TABLE 4: Relative Energies (eV) for the Electronic States of All the Considered Complexes[a]

	gas phase				solution			
	S0	T1		S1	S0	T1		S1
		ΔSCF	TDDFT	TDDFT		ΔSCF	TDDFT	TDDFT
				$M(bpy)_2(CN)_2$				
Ru	0.0	1.60 (1.45)	1.46	2.33	0.0	2.15 (1.98)	2.02	2.59
Os	0.0	1.39 (1.25)	1.48	2.31	0.0	1.99 (1.88)	2.10	2.57
				$M(bpy)_2(NCS)_2$				
Ru	0.0	1.35 (1.16)	1.21	2.24	0.0	1.90 (1.74)	1.80	2.57
Os	0.0	1.17 (0.96)	1.10	2.37	0.0	1.64 (1.50)	1.51	2.48

[a] All the values have been computed using ground-state geometries, except for the values reported in parenthesis, which have been computed using optimized triplet geometries.

The S0/T1 vertical gaps, obtained by freezing the geometry of the ground S0 state, are 1.6 eV for *cis*-$Ru(bpy)_2(CN)_2$ and 1.4 eV for the corresponding osmium complex. Lower energies (by about 0.2 eV) are, instead, found for the triplet states of the thiocyanate compounds. This difference can be rationalized in terms of the HOMO shape: in the thiocyanate complex this orbital has a significant antibonding M−N contribution, which decreases upon excitation of one electron (see Figure 3).

Optimizations of the geometries of the triplet states decrease the excitations gap by about 0.1 eV for the cyanide and by 0.2 eV for the thiocyanate complexes (see Tables 5 and 6), and small differences are found in the geometrical parameters. For instance, the C3C4 bond distance decreases in the triplet state (acquiring a partial double bond character), whereas the N2C3 length increases. In general, all the geometrical variations are consistent with the occupation of the π^* orbitals of the pyridyl ligands depicted in Figure 3, and the variation path follows the bonding/antibonding scheme in such plots.

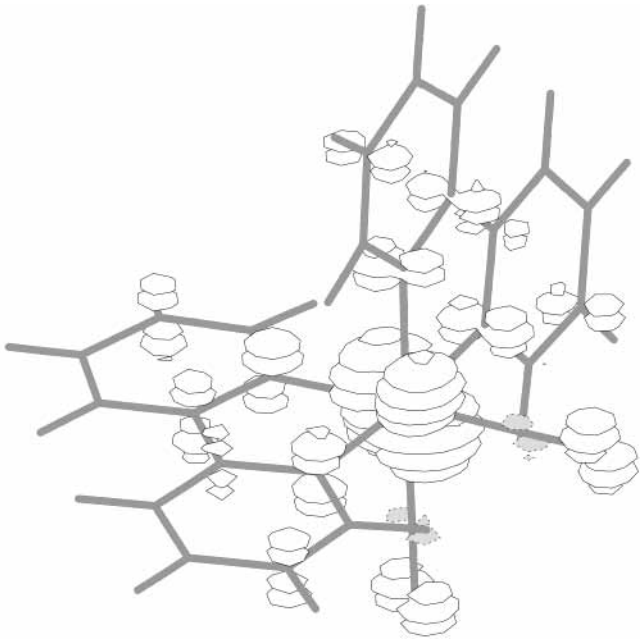

Figure 4. Spin density map for the triplet state of $Ru(bpy)_2(CN)_2$.

TABLE 5: Main Geometrical Parameters (Ångstroms and Degrees) of the Lowest Triplet State of the $M(bpy)_2(CN)_2$ (M = Ru and Os) Complexes[a]

	M = Ru		M = Os	
$M(bpy)_2CN_2$	gas	aq soln	gas	aq soln
MN2	2.116	2.110	2.102	2.112
C1N2	1.359	1.358	1.363	1.364
N2C3	1.390	1.390	1.392	1.381
C3C4	1.452	1.453	1.448	1.474
C4N5	1.393	1.393	1.396	1.384
N5C6	1.363	1.363	1.368	1.369
MN5	2.081	2.081	2.066	2.080
MC7	2.023	2.022	2.008	1.980
C7N8	1.193	1.193	1.194	1.190
MN2C3	114.4	114.5	114.9	115.5
MN2C1	125.8	125.3	125.5	125.5
MN5C4	115.4	115.2	116.0	116.3
MN5C6	124.9	125.0	124.7	124.9
C7MN5	95.4	95.6	95.0	94.6
N2C3C4N5	2.7	2.8	2.7	0.3

[a] All values have been computed at the PBE0 level using the CEP-121G basis.

It is noteworthy that TDDFT computations, carried out at S0 geometries (see column 4 in Table 4), give quite small differences (about 0.1 eV) with respect to ΔSCF computations, thus pointing out the one-electron nature of these excitations.

For what concerns the structure of the triplet states, in going from the gas phase to the solution, the same trends observed for the singlet ground state are found, with a general contraction of all the metal−ligand (CN^- or SCN^-) bond lengths. At the same time, the solvent increases the gap between S0 and T1 states, the effect being larger for the cyanide complexes than for the thiocyanate ones. In particular, the S0/T1 gap is around 2 eV for the *cis*-$Os(bpy)_2(CN)_2$ (1.4 eV in the gas phase) and 1.6 eV (1.2 eV in the gas phase) for the *cis*-$Os(bpy)_2NCS_2$, thus underlining the larger electronic rearrangement in the cyanide complexes encountered for the singlet state.

3.3. Electronic Spectra. Finally, we have computed the UV spectra, both in the gas phase and in solution, using a TD-DFT approach. All these vertical electronic transitions have been evaluated at the corresponding gas phase or solution geometries of the singlet (S0) ground electronic state, and the results are collected in Table 7. In the table we have reported only the active bands that are those important for a complete characterization of the complexes. Lower excitations, corresponding essentially to inactive d−d transition have been also computed, but being not important for the photochemical process under investigation, they have not been reported.

TABLE 6: Main Geometrical Parameters (Ångstroms and Degrees) of the Lowest Triplet State of the $M(bpy)_2(NCS)_2$ (M = Ru and Os) Complexes[a]

	M = Ru		M = Os	
$M(bpy)_2NCS_2$	gas phase	aq soln	gas phase	aq soln
MN2	2.077	2.163	2.055	2.062
C1N2	1.360	1.367	1.366	1.372
N2C3	1.391	1.381	1.397	1.412
C3C4	1.453	1.488	1.447	1.459
C4N5	1.391	1.389	1.395	1.413
N5C6	1.361	1.372	1.366	1.374
MN5	2.077	2.154	2.059	2.053
MN7	2.000	1.931	1.991	1.948
N7C8	1.198	1.186	1.198	1.188
C8S9	1.671	1.657	1.668	1.659
MN2C3	114.7	114.8	115.1	114.4
MN2C1	125.5	126.0	125.5	126.5
MN5C4	114.9	114.5	115.2	114.6
MN5C6	125.3	126.8	125.4	126.8
N7MN5	94.2	93.3	94.2	93.5
N2C3C4N5	1.2	0.1	0.7	1.3

[a] All values have been computed at the PBE0 level using the CEP-121G basis.

All the complexes show two strong absorption bands, one centered at about 380/400 nm and another one at lower energy, around 500/530 nm.[36] As expected, both transitions are well described by the TDDFT approach, even if the first transition is systematically underestimated and the second overestimated. Furthermore, our results well agree with some previous semiempircal calculations on the *cis*-$Ru(bpy)_2(NCS)_2$ complexes.[14]

All these transitions are dominated by MLCT bands, corresponding to a single excitation from a d orbital of the metal to a π^* orbital of the ligand. In particular, the lowest band corresponds to an HOMO/LUMO excitation (see Figure 3 for the shape of such orbitals), whereas the higher involves a lower d orbital (HOMO−2) and a higher empty π^* orbital (LUMO+2 or higher). The latter is a compact π^* orbital localized on only one ring of each bipyridyl ligand.

Our calculations also reproduce (even if not quantitatively) the red shift observed in going from Ru to Os complexes having identical chemical environments. This variation is consistent with the decrease of electron density on the metal resulting in a destabilization of its partially filled d orbitals, the Os atom always bearing a larger positive charge than Ru (refer to the atomic charges in Table 3).

In the same table are reported the oscillator strengths for the considered transitions. It clearly appears that larger basis sets would be needed for the evaluation of vertical excitation to obtain converged oscillator strengths.[54] Nevertheless, some indications can be drawn from our values as well. For instance, the oscillator strengths are higher in cyanide complexes than in the thiocyanate ones, in agreement with the experimental findings.[36]

In going from the gas phase to aqueous solution, we can observe a small variation (±10/15 nm) for the lower energy band, whereas the highest bands are all significantly blue-shifted (−50/60 nm). Both shifts improve the agreement with the experimental data. The different magnitudes in the solvent shifts arise from the different nature of the virtual orbitals involved,

TABLE 7: Computed TDDFT Vertical Excitation Energies (nm) for the Lowest Singlet and Triplet States of All the Considered Complexes[a]

		Ru			Os		
	transition	gas phase	aq soln	exp[b]	gas phase	aq soln	exp[b]
$M(bpy)_2CN_2$	S0 → S1	357 (0.08)	367 (0.06)	376	364 (0.14)	370 (0.13)	382
	S0 → S2	532 (0.13)	478 (0.17)	496	538 (0.14)	487 (0.17)	508
	S0 → T1	849 (0.0)	614 (0.0)		892 (0.0)	623 (0.0)	≈680
$M(bpy)_2NCS_2$	S0 → S1	412 (0.08)	397 (0.02)	398	427 (0.03)	415 (0.02)	412
	S0 → S2	554 (0.02)	482 (0.09)	538	546 (0.04)	498 (0.09)	530
	S0 → T1	1025 (0.0)	689 (0.0)		1060 (0.0)	756 (0.0)	≈780

[a] All values have been computed using the ground state geometries. [b] Reference 36.

because both excitations are generated from similar d orbitals. In fact, solvent has the strongest effect on the LUMO orbital, which is more delocalized, and so more polarizable, than on higher, more compact, virtual orbitals.

Apart for the red shifts discussed above, the Os complexes experimentally show an additional absorption band at longer wavelength than the Ru complexes. This lower energy transition has been supposed to be an electronic transition between the ground and the triplet excited state of the Os compounds, allowed by spin−orbit coupling.[36] In addition, this band is red-shifted when the ligand is changed from CN^- to SCN^-. Looking at Table 7, a good agreement between the computed S0/*T*0 transition and the reported experimental band can be found. At the same time, our computations reproduce also the red shift observed when going from cyanide to thiocyanate. As for the shift between Ru and Os, this effect is related to the depletion of electron density on the metal atom.

Finally, we want to stress that our DFT calculations do not take spin−orbit effects into account, which are not included in current TDDFT approaches. Spin−orbit coupling is responsible for the mixing of singlet and triplet states, allowing the latter to acquire intensity in both absorption and emission and, at the same time, favors the decay from the excited singlet.[36,53] An additional effect is that the triplet energies are shifted, upon coupling with higher states: for the third row transition metals this effect should not be larger than 0.2/0.3 eV, and even less for the second row atoms.

4. Conclusion

In this paper, we have applied a recent DFT method to analyze ground and excited-state properties of some dyes used in photovoltaic applications. These systems, of general formula *cis*-$M(bpy)_2L_2$ (M = Ru, Os and L = CN and SCN), have been studied both in the gas phase and in aqueous solution, miming the solvent with a dielectric continuum model. Electronic spectra have been simulated, both in gas phase and in solution, using a TDDFT approach. Apart from the good agreement with the experimental findings for what concerns structural and electronic properties, our results explain the differences observed for these complexes in changing the central metal atom (Ru vs Os), the chemical environment (CN vs SCN), or the medium (gas phase vs solution). The main conclusions can be summarized as follows:

Ruthenium and osmium provide similar electronic properties for the ground states, whereas larger differences have been found for the T1 and S1 states.

Cyanide and thiocyanate ligands sligthly alter the spectral absorption of the complexes. Furthermore, they cause important modifications in the S0 state, thus pointing to a different role in the redox reaction taking place after the light absorption.

The solvent effect is mainly to stabilize charge separation and, therefore, induces significant modifications on the electronic structures of the considered complexes, and, to a lesser extent, on the geometrical parameters.

The most remarkable solvent effect is a significant stabilization of structures involving a formal charge separation, which induces not negligible modifications on the electronic structures of the considered complexes and, to a lesser extent, on their geometrical parameters.

Both the first singlet and triplet excited states (S1 and T1) can be described mainly as one electron excitations.

The red shift observed in going from Ru to Os transitions can be ascribed to the destabilization of the d orbitals upon partial electronic depletion. At the same time, the additional band detected for Os compounds at low energy has been confirmed to be a S0/T1 transition.

Due to the great chemical and industrial interest of such dyes, we hope that our results help to rationalize the experimental observations and, at the same time, suggest some hints for new complexes with improved photochemical behavior.

Acknowledgment. We thank CNRS for a financial support in the framework of the ACI "Jeune Equipe 2002" project.

References and Notes

(1) Hagfeldt, A.; Gratzel, M. *Acc. Chem. Res.* **2000**, *33*, 269. Graetzel, M.; Reagan, B. O. *Nature* **1991**, *353*, 737.

(2) Rudmann, H.; Shimada, S.; Rubner, M. F. *J. Am. Chem. Soc.* **2002**, *124*, 4918.

(3) Gao, F. G.; Bard, A. J. *J. Am. Chem. Soc.* **2000**, *122*, 7426.

(4) Balzani, V.; Juris, A. *Coord. Chem. Rev.* **2001**, *211*, 97.

(5) Nazeeruddin, Md. K.; Pechy, P.; Renouard, T.; Zakeeruddin, S. M.; Humphry-Baker, R.; Comte, P.; Liska, P.; Cevey, L.; Costa, E.; Shklover, V.; Spiccia, L.; Deacon, G. B.; Bignozzi, C. A.; Gratzel, M. *J. Am. Chem. Soc.* **2001**, *123*, 1613.

(6) Cahen, D.; Grätzel, Guillemoles, J. F.; Hodes, G. In *Electrochemistry of nanomaterials*; Hodes, G., Ed.; Wiley-VCH: Weinheim, Germany, 2001.

(7) Tachibana, Y.; Moser, J. E.; Grätzel, M.; Klug, D. R.; Durrant, J. R. *J. Phys. Chem.* **1996**, *100*, 20056.

(8) Treadway, J. A.; Moss, J. A.; Meyer, T. *J. Inorg. Chem.* **1999**, *38*, 4386.

(9) Ellingson, R. J.; Asbury, J. B.; Ferrere, S.; Ghosh, H. N.; Sprague, J. R.; Lian, T.; Nozik, A. J. *J. Phys. Chem. B* **1998**, *102*, 6455.

(10) Kuciauskas, D.; Freund, M. S.; Gray, H. B.; Winkler, J. R.; Lewis, N. R. *J. Phys. Chem. B* **2001**, *105*, 392.

(11) Zheng, K.; Wang, J.; Shen, Y.; Kuang, D.; Yun, F. *J. Phys. Chem. A* **2001**, *105*, 7248.

(12) Damrauer, N. H.; Weldon, B. T.; McCusker, J. K. *J. Phys. Chem. A* **1998**, *102*, 3382.

(13) Wolfbauer, G..; Bond, AM..; Deacon, G. B.; MacFarlane, D. R.; Spiccia L. *J. Am. Chem. Soc.* **2000**, *122*, 130−142

(14) Rensmo, H.; Lunell, S.; Siegbahn, H. *J. Photochem. Photobiol. A* **1998**, *114*, 117.

(15) Shinozaki, K.; Takahashi, N. *Inorg. Chem.* **1996**, *35*, 3917.

(16) Albano, G.; Belser, P.; Daul, C. *Inorg. Chem.* **2001**, *40*, 1408.

(17) Nazeeruddin, Md. K.; Zakeeruddin, S. M.; Humphry-Baker, R.; Gorelsky, S. I.; Lever, A. B. P.; Gratzel, M. *Coord. Chem. Rev.* **2000**, *208*, 213

(18) Koch, W.; Holthausen, M. C. *A Chemist's Guide to Density Functional Theory*; Wiley-VCH: Weinheim, Germany, 2000.

(19) Adamo, C.; di Matteo, A.; Barone, V. *Adv. Quantum Chem*. **1999**, *36*, 4.
(20) Runge, E.; Gross, E. K. U. *Phys. Rev. Lett.* **1996**, *76* 1212.
(21) Bauernschmitt, R.; Ahlrichs, R. *Chem. Phys. Lett.* **1996**, *256*, 454.
(22) Casida, M. K.; Jamorski, C.; Casida, K. C.; Salahub, D. R. J. *Chem. Phys.* **1998**, *108*, 4439.
(23) Stratmann, R. E.; Scuseria, G. E.; Frisch, M. J. *Chem. Phys.* **1998**, *109*, 8128.
(24) Tozer, D. J.; Handy, N. C. *J. Chem. Phys.* **1998**, *109*, 10180.
(25) Matsuzawa, N. N.; Ishitani, A.; Dixon, D. A.; Uda, T. *J. Phys. Chem. A* **2001**, *105*, 4953.
(26) Boulet, P.; Chermette, H.; Daul, C.; Gilardoni, F.; Rogemond, F.; Weber, J.; Zuber, G. *J. Phys. Chem. A* **2001**, *105*, 885.
(27) Cavillot, V.; Champagne, B. *Chem. Phys. Lett.* **2002**, *354*, 449.
(28) Perdew, J. P.; Burke, K.; Ernzerhof, M. *Phys. Rev. Lett.* **1996**, *77*, 3865; *ibid* **1997**, *78*, 1396.
(29) Adamo, C.; Barone, V. *J. Chem. Phys.* **1999**, *110*, 6158.
(30) Adamo, C.; Barone, V.; Scuseria, G. E. *J. Chem. Phys.* **1999**, *111*, 2889.
(31) Adamo, C.; Barone, V. *Chem. Phys. Lett.* **2000**, *330*, 152.
(32) Adamo, C.; Barone, V. *Theor. Chem. Acc.* **2000**, *105*, 169.
(33) Barone, V.; Fabrizi de Biani, F.; Ruiz, E.; Sieklucka, B. *J. Am. Chem. Soc.* **2001**, *123*, 10742.
(34) Gerfin, T.; Gratzel, M.; Walder, L. *Prog. Inorg. Chem.* **1997**, *44*, 345.
(35) Nazeeruddin, M. K.; Kay, A.; Rodicio, I.; Humphry-Baker, R.; Muller, E.; Liska, P., Vlachopoulos, N. Gratzel, M. *J. Am. Chem. Soc.* **1993**, *115*, 6382.
(36) Sauvé, S.; Cass, M. E.; Coia, G.; Doig, S. J.; Lauermann, I.; Pomykal, K. E.; Lewis, N. S. *J. Phys. Chem. B* **2000**, *104*, 6821.
(37) Shklover, V., Nazeeruddin, M. K.; Zakeeruddin, S. M.; Barbé, C.; Kay, A.; Haibach, T.; Steurer, W.; Hermann, R.; Nissen, H. U.; Grätzel, M. *Chem. Mater.* **1997**, *9*, 430.
(38) Shklover, V., Ovchinnikov, Y. E.; Braginsky, L. S.; Zakeeruddin, S. M.; Grätzel, M. *Chem. Mater.* **1998**, *10*, 2533.
(39) Frisch, M. J.; Trucks, G. W.; Schlegel, H. B.; Scuseria, G. E.; Stratmann, R. E.; Burant, J. C.; Dapprich, S.; Millam, J. M.; Daniels, A. D.; Kudin, K. N., Strain, M. C.; Farkas, O.; Tomasi, J.; Barone, V.; Cossi, M.; Cammi, R.; Mennucci, B.; Pomelli, C.; Adamo C.; Clifford, S.; Ochterschi, J.; Cui, Q.; Gill, P. M. W.; Johnson, B. G.; Robb, M. A.; Cheeseman, J. R.; Keith, T.; Petersson, Morokuma, K.; Malick, D. K.; Rabuck, A. D.; G. A.; Montgomery, J. A.; Raghavachari, K.; Al-Laham, M. A.; Zakrewski, V. G.; Ortiz, J. V.; Foresman, J. B.; Cioslowski, J.; Stefanov, B. B.; Nanayakkara, A.; Liu, J.; Liashenklo, A.; Piskorz, P.; Komaromi, I.; Challacombe, M.; Peng, C. Y.; Ayala, P. Y.; Chen, W.; Wong, M. W.; Andres, J. L.; Replogle, E. S.; Gomperts, R.; Martin, R. L.; Fox, D. J.; Binkley, J. S.; DeFrees, D. J.; Baker, J.; Stewart, J. P.; Head-Gordon, M.; Gonzalez, C.; Pople. J. A. *Gaussian 99*, Revision B.5; Gaussian, Inc.: Pittsburgh, PA, 1998.
(40) Adamo, C.; Barone, V. *Chem. Phys. Lett.* **1997**, *272*, 242.
(41) Frisch, Æ.; Frisch, M. J. *Gaussian 98 User's Reference*; Gaussian, Inc.: Pittsburgh, PA, 1998 (see also references therein).
(42) Couty, M.; Hall, M. B. *J. Comput. Chem*. **1996**, *17*, 1359.
(43) Tomasi, J.; Persico, M. *Chem. Rev.* **1994**, *94*, 2027.
(44) Barone, V.; Cossi, M.; Tomasi, J. *J. Chem. Phys*. **1997**, *107*, *3210*.
(45) Barone V.; Cossi, M. *J. Phys. Chem. A* **1998**, *102*, 1995.
(46) Cossi, M.; Barone, V. *J. Chem. Phys.* **2001**, *115*, 4708.
(47) Bader, R. F. W. *Atoms in Molecules: A Quantum Theory*; Oxford University Press: Oxford, U.K., 1990.
(48) Noury, S.; Krokidis, X.; Fuser, F.; Silvi, B. *Comput. Chem.* **1999**, *23*, 597.
(49) Kallioinen, J.; Benko, G.; Sundström, V.; Korppi-Tommola, J. E. I.; Yartsev, A. P. *J. Phys. Chem. B* **2002,** *106*, 4396.
(50) Cheng, J. K.; Cheung, K. K.; Che, C. N. *Chem. Commun.* **1997**, *6*, 623.
(51) Kohle, O.; Ruile, S.; Grätzel, M. *Inorg. Chem*. **1996**, *35*, 4779.
(52) Dewar, M. J. S. *Bull. Soc. Chim. Fr.* **1951**, *18*, C71
(53) Chatt, J.; Duncanson, L. A. *J. Chem. Soc.* **1953**, 2939.
(54) Wiberg, K. B., Stratmann, R. E., Frisch, M. J. *Chem. Phys. Lett*. **1998**, *297*, 60.